Section A-Research paper
ISSN 2063-5346

Formulation and evaluation of charantin loaded nanoemulsion based gel for its antidiabetic efficacy

Mohammad Rashid[1, 3], Farhan J Ahmad[2], Sanjar Alam[3], Rakesh K Sindhu[1*]

[1]School of Pharmacy, Sharda University, Greater Noida, U.P.

[2]Department of Pharmaceutics, School of Pharmaceutical Education & Research, Jamia Hamdard, New Delhi, 110062.

[3]R.V. Northland Institute, G.B. Nagar, Dadri, Greater Noida. U.P.-203207

***Corresponding Author**

Dr. Rakesh K Sindhu
Professor
School of Pharmacy
Sharda University,
Greater Noida-U.P. 201306
rakesh.kumar7@sharda.ac.in
M. No- 9540324534

1. Introduction

If action or secretion of Insulin hormone is detracted, its consequence seen as Diabetes mellitus (DM). Its initial characteristic is hyperglycemia i.e., high blood glucose level from slandered limits and if glucose label remains unmanaged for long term, many complication of kidney, heart, nervous systems start to develop, these are called as secondary effects over the body. (Egan and Dinneen 2019) (Canadian Journal of Diabetes, 2018).

According to Global report on diabetes by WHO-2016, 9.24 million/year is the rate of its spreading from 1980 to 2014 in general population while in adults it is spreading with the rate of "4.7% in 1980 to 8.5% in 2014" (World Health Organization 2016). According to International Diabetes Federation (IDF) the current load of diabetic people over world is 425 million and till 2045 it is estimated to be doubled in parallel to this the load of diabetic people in South East Asia (SEA) 82 million, i.e. 19.29% of total diabetics of world & till 2045 the estimation is there will be burden of 151 million diabetics from SEA. As per IDF reports, till 2017 there was about 73 million cases of diabetes in India. Diabetes inserts burden over region, country and ultimately over glove in the form of money, manpower and mental stress. The above data is alarming situation as epidemic scenario of diabetes and parallel to it there

is going to develop many secondary body complications like CVDs, Renal disorders & eye blindness etc. (Habtemariam 2019).

Low glucose due to DM in cells & organs affects working efficiency side by side high glucose label in blood and fluids of organs attracts infections and organ destruction. (Egan and Dinneen 2014). DM can be diagnosed as if the blood glucose label is beyond the limit as in Daytime range from 80-120 mg/dL, Bed time (in night) range from between 100-140 mg/dL & HbA1c levels-7% (Simona et al. 2017).

The oral hypoglycaemic drugs like Metformin, Glimepiride, Glipizide, Glibenclamide, Gliclazide, Pioglitazone, Rosiglitazone, etc are of synthetic drugs and are associated with poor aqueous solubility so have poor bioavailability consequently have higher effective dose with side effects (Khursheed et al. 2019). In last 9-10 years of research records, DM 49% therapeutic planning's are of Herbal origin (Gothai et al. 2016). There are challenges with bioactive herbal Antidiabetic agents. These are less efficacious and show lean bioavailability by oral route of administration due to digestive actions in GIT, transport, absorption & solubility issues. These are bypassed by using Novel and advanced drug delivery systems. (Ganesan, Arulselvan, and Choi 2017). In advance pharmaceutical technologies Nano-carriers are most efficient for bioavailability improving over solubility, stability and permeability issues of drugs, over regular-common drug delivery system. (Harwansh et al. 2015). Nanogel of herbal bioactive agents applied via TDDS (trans dermal drug delivery system) are reported to give controlled, sustained & best permeation rates, bypasses the hepatic degradation (Azeem et al. 2012).

Therefore, the rationale of planning the formulation with selected administration route in this study as nanoemulsion based Nanogel for TDDS use is to revamp the therapeutics & effectiveness of herbal drug and minimizing their toxicity, complications and implications.

2. Materials and methods:

2.1. Chemicals and excipients:

Charantin (CRT) was bought from Sigma Aldrich, Bangalore. Propylene glycol caprylate (Sefsol 218®), Isopropyl myristate (Stepan D 50), Glycerol Triacetate (Triacetin), Glycerol monooleate (Peceol®), Fractionated coconut oil (Miglyol 812®), Labrafac® was taken a gift sample. Polyoxy-35-castor oil (Cremophore), Tween 80, Tween 20, Lab rasol, Trans cutol, Plurol-Oleique was obtained from R. V. Northland Institute, Grt. Noida. Some analytical grade reagents and chemicals obtained from Merckindustries, Bombay-India. Milli-Q-water used.).

2.2. Molecular Docking:

The Maestro 10.5 program was used this study called as ligand docking study. The specification of this maestro program was, "Schrodinger Inc. USA, Intel (R) Core (TM) i3-2400 CPU @ 2.40 GHz, 4 GB RAM, OS 64 bit. The Tyrosine kinase receptor in crystalline 3D structure was obtained from Protein-data-bank (PDB). The PDB-Id was used-1FM9 (Bhutani et al. 2018)(Bhutani et al. 2019). The obtained protein from bank was designed software in three steps "i.e." preprocess, optimize and minimize using protein preparation wizard. Those water molecules deleted which can alter the result by interacting with the receptor and side by side the hydrogen atoms which were missing were added. The OPLS 2005 force field was used to trace and optimise the structure's energy. The receptor grid box was created using a programme called receptor grid generation program. The ligands were docked in this box. The results obtained were analysed based on their docking scores.

2.3. MMGBSA:

Prime MM-GBSA DG binding method was used to find the binding energy of ligands, with the help of Maestro 10.5 (Schrodinger Inc. USA) software (Husain et al. 2021). This approach uses docking results as the primary source of data, and binding energy calculations were made. Binding energy is the result of various biomarker interactions with the receptor in the pocket, including electrostatic contacts, polar interactions, hydrophobic interactions, van der Waals interactions, and - π-π stacking, among others. Numerous types of interactions sum-up to total binding energy which denotes the stability of a molecules in the active pocket present in target receptor. Binding energy (negative value) is used as stability marking in proportion.

2.4. Preformulation Studies:

2.4.1. *Drug Characterization:*

Drug sample was characterized by its physiochemical properties such as color, odor, taste & solubility in water and the results were recorded. UV- spectroscopic scanning through 200-400 nm λ was done. Drug concentration of 0.01% w/v dissolved in solvent (methanol: phosphate buffer 0.05M & pH 7.4 in ratio 70:30) and UV spectroscopy by-Shimadzu-UV-1700 Corporation Kyoto Japan was done. Further FTIR scanning was done of drug with Potassium bromide (KBr) the ratio of (100:1) pellet, recorded on 1520 (Shimadzu, Japan). FTIR studies was also performed to report if there is any chemical interactions between CRT and excipients (FTIR measuring over range of 4000-450 cm-1).

2.4.2. *RP-HPLC analysis of drug (CRT):*

For chromatographic analysis of drug was done by using by a Shimadzu model HPLC. The HPLC was working with CLASS-VP 5.032 software. The HPLC has quaternary LC-10AVP pumps and UV/VIS detector. The column was SPD-10AVP & SCL 10AVP system controller (Shimadzu). For sample injection, 'Rheodyne injector fitted with a 20 µL loop' was added. During analysis, flow rate settled 1.2 mL/min with 15 min run time adjusted. The UV detector was at 278 nm at 25 ± 0.5°C. 20 µL micro-syringe (Hamilton Microliter®; Switzerland) was used sample ingestion as Load.

The drug CRT was solubilised in methanol having concentration (1000 µg/ml), marked as stock solution. The dilutions 2, 4, 6, 8, 10, 12, 14, 16, 18, 20 µg/ml was developed by serial dilutions with same solvent. These stored at 4°C and away from light. The mobile phase used was Acetonitrile: water-deionised (75:25 v/v) used as mobile-phase which was adjusted with pH=2.3 by using adding 1% glacial acetic acid. The mobile phase was properly sonicated for 15 min and made it free from gases prior to use. The dilutions were passed through 0.45 µm filter (NYL) syringe then only inserting in HPLC.

2.4.3. *Screening of Excipients:*

CRT with excess amount, was dispersed in 2 mL of solvents [oil, surfactants (S), co-surfactants (Co-S) and distilled water) taken in separate and marked 5 ml capacity stopper vials. The dispersions were mixed on vertex mixture and equilibrated (for 72 hrs. at 25±1.0 ^{0}C) in isothermal shaker. Each vials was centrifuged at 3000 rpm for 15 min (Spinwin MC-02, Tarson. India), the supernatant was applied in RP-HPLC at λmax 278 nm after filtering through 0.45 µm membrane filter, for solubility (S. Alam et al. 2010).

2.5. preparation of nanoemulsion(NE) :

2.5.1. *Optimisation of Nanoemulsion composition:*

Diverse ratios of NEs were designed and for each ratio, phase diagrams were devised to find out optimised ratios from the NE regions. Visual observation was done, if transparent and easily flow able o/w NEs were obtained we marked it o/w NE. The oil phase included precisely 2% w/w of CRT, which was kept constant in all the chosen NEs, and these were then put through several thermodynamic stability experiments.

2.5.2. *Selection of NEs by Thermodynamic Stability Studies:*

For selection of stable formulations following tests were performed (S. Alam et al. 2010):

1. Centrifugation test: The selected NEs observed for any phase separation after applying centrifugation (at 35, 00 rpm for 30 minutes). The NEs which were stable (no any phase separations seen) taken for the heating and cooling cycle.
2. Heating-Cooling Cycles: Six heating-cooling cycles, with storage at each temperature for at least 48 hours, were used, with the lowest temperature being 4 °C and the maximum being 45 °C. The NEs that proved to be stable under these stresses were chosen for the freeze-thaw cycle test.
3. Freeze-thaw cycles: The NEs that survived thermodynamic stability testing of three freeze-thaw cycles between -21 0C and +25 0C storage at each temperature for not less than 48 hours were chosen for further investigation.

2.6. Characterization of Nanoemulsions:

To identify and selection of optimal NE for best in-vivo actions the characteristics are evaluated like droplet size, viscosity, RI, percentage transmittance (%T), Transmission Electron Microscopy (TEM). Minimised size of globules assists translucent or transparent appearance as this globule size allows higher transmission of the light (Fernandes et al. 2021).

2.6.1. *Micromeretic study and zeta potential analysis:*

The thermodynamically stable NEs were scanned for optimisation by micromeretic properties like Dropletsize (Z-average) & polydispersityindex (PDI), these were measured by photon-correlation-spectroscopy (PCS) using a Malvern-Zeta-sizer (Nano ZS90, Malvern instruments Ltd., UK) with a 50 mV laser. 0.1ml emulsion was thoroughly mixed in 50ml of water in a volumetric flask and scattering of light was measured at 90^0 angle. At least three measurements were performed for each droplet size value reporting and their average was used with SD (Mustafa et al. 2012). Structure and surface morphology of the droplets of NE were scanned using transmission electron microscopy (TEM-with Topcon 002 B at 200 kilo Volt, mfg. by Topcon Paramus, NJ). The procedure for TEM was by taking a drop of the NE and directly applying on the holey film grid. The observations recorded (Sanjar Alam et al. 2012).

2.6.2. *Rheological studies of NEs:*

0.5 g NE was taken in Brookfield DV III ultra V6.0 RV cone and plate viscometer at 25 ^{0}C ± 0.3 ^{0}C for viscosity measurement. The flow behaviour was evaluated in Rheometer (Anton Paar, Modular Compact -MCR 102). The measurements were performed at a temperature of 25 ± 0.5°C with a 4°/40 mm cone and plate geometry and gap of 0.100 mm. The steady of

rheological behaviour of the nanogel (CRT-NG) and placebo were also performed at a controlled rate (from 0.001 – 100 and 0.0001 – 100 s^{-1} respectively). The samples were allowed to rest about 10 minutes prior to measurement after applying in Rheometer (Chaudhari and Kuchekar 2018).

2.6.3. *Refraction Index(RI) & pH Measurements:*

RI & pH were determined in triplicate for both placebo and drug-loaded NEs by using Abbe-refractometer (NIRMAL-International) and PH-meter (Mettler Toledo MP 220, Greifensee, Switzerland) respectively at 25°C (Shakeel et al. 2007) .

2.6.4. *Selection of optimised formulation by release kinetics study:*

Each group of nanoemulsion and finally optimised nanogel was applied in the USP- XXIV rotating paddle dissolution apparatus (DS8000, Lab India, India). The samples are put in dialysis membrane pouches, mounted in a flask with buffer at 37±0.5°. 50 rpm was used stirring speed in experiment. The % Drug release at fixed time intervals is recorded from sample's withdrawn. The CRT content using was evaluated by validated HPLC method at 278 nm absorbance and at calibration curve (Sultana et al. 2012).

2.6.5. *CRT permeation study trough rat-skin:*

Abdominal (Hairless) skin exposing stratum corneum donor compartment and dermis towards accepting section (filled with phosphate buffer saline, pH 7.4) was mounted in the Franz diffusion cell. The area effective for diffusion was 1.765 cm^2. The 37 ± 0.5°C temperature of diffusion cell was maintained with constant magnetic stirring. NE applied evenly over the skin in donor section of Franz-diffusion cell and occlusive conditions are created by sealing with paraffin film. A 200 µL sample from receptor buffered medium was taken out at fixed time intervals over a period of 24 h, and an equal volume of fresh buffered medium was drained into to maintain the experimental conditions. All samples were filtered, diluted and analysed by RP-HPL at 278 nm (n=3).(Azeem, Ahmad, et al. 2009)

For analysis of data, the Cumulative amount of drug permeation **(CDP)** (µg/cm^2) through mounted - skin in diffusion cell was plotted with respect to time (t, h). The plot was straight line with slope equals to flux (Jss, µg/ cm2/h), the intercept of plot is the lag time (t_L, h). The enhancement ratio (ER) was calculated.

2.7. Transforming the optimised nanoemulsion into nanogel and it's characterisation:

To improve the compliance of dermal application the optimised NE (CRT-NE4G) was transformed to Hydrogel by using Carbopol 934. This is gelling agent and is biocompatible, biodegradable, bioadhesive, non-irritating and no body-absorption reported. (Aiyalu,

Govindarjan, and Ramasamy 2016). Dispersed the carbopol-934 (1 g) in 100 ml distilled water and stored (25^0C) in the dark place for 24 h till it swelled completely. The optimised CRT-NG was mixed with 1 g of an already swollen carbopol 934 dispersion system to create a homogenous mass, which was developed as NE gel (CRT-NG, 0.1 g of CRT). Triethanolamine, a neutralising mixture was added to neutralize the carbopol. The developed nanogel was evaluated for various parameters (Barkat et al. 2017).

Charantin was adding in carbopol dispersion having 0.5% w/w of Triethanolamine as neutralising mixture directly, finally make-up the volume 100ml, labelled as Neat formulation Conventional Gel of CRT (NF^{cg}) (Azeem, Rizwan, et al. 2009).

2.8. Stability Assessment of Nanogel

The optimized nanogel (CRT-NG) was put at long accelerated stability testing. The ICH recommended parameters (40±2 °C/75±5% RH). The glass vials used to store the nanogel were airtight. Physicochemical, distinctive features (appearance, precipitation, clarity, pH, droplet size, zeta potential), and drug content were assessed at intervals of 0, 1, 3, and 6 months. Drug content was quantified by using RP-HPLC method at 278 nm. The shelf life (t_{90}) was predicted by plotting the Log-Percentage of the remaining drug with respect to time.

2.9. In-Vivo Study

2.9.1. *Study-Animals*

Wistar-albino rats (male of 180-220 g weight) were selected and divided in six groups (n=6). The ambient temperature 25 ± 0.5°C and 45-55% R.H was maintained with 12.0 hr. light/dark cycles. The work on animals as per plan was done as per approval of the Institutional Animal Ethical Committee with the ethical guidelines provided by the committee (approval number: RVNI/IAEC/2021/01) via CPCSEA, India.

2.9.2. *Antidiabetic Efficacy study of the CRT loaded Nanogel:*

Sustaining antidiabetic action of the optimized nanogel was evaluated by the method developed by in Wistar rats by Winter et al. Diabetes was induced by the single intra peritoneal (i. p.) dose (250 mg/kg) administration of streptozotocin solution in citrate buffer (pH 4.5) in rats, fasted-16 hours. The Induction of Diabetes is confirmed if-Polydipsia, Polyuria and Blood glucose label >200 mg/dl, observed after 72 hrs. since injection of STZ, then selected for experiment.

Experimental design-

30 Animals are taken in 5 Groups on random basis (Arora et al. 2023)

Group I*:* Normal (Non-Diabetic) animals – Standard Control group.

***Group II**:** Control (Diabetic) animals-Toxic group OR Negative Control group.

Group III: Reference standard drug (receiver) - Positive Control Group.

Groups IV & V: Receiver of the Optimized Formulation.

**Receiver of vehicle only, (Arora et al. 2023).

The calculated dose for the rats was applied over shaved area of abdominal region of rat. Shaving was done 12 hrs. before the experiment starts. Blood glucose level was estimated in fasting conditions by puncturing the tail vein, using Glucometer (Accutrend GC of Roche reactive strips of Accu-Chek).

2.9.3. Skin Irritancy Test:

Scored the of skin irritancy as 0-1-2-3 during skin irritancy test as per Aqil et al. A 10 µL of the nanogel was applied to the left ear, with the right ear was control of animals, which are kept at standard conditions. Erythema and Oedema was monitored during six days of application.

2.10. Data analysis by statistical method:

ANOVA was applied followed by Dun net's test using Graph Pad Prism software-5.0 (San Diego, CA, USA). The significance of difference was tested at $P < 0.05$ between the means.

3. RESULT & DISCISSION

3.1. Docking Study:

3.1.1 Molecular Docking:

The docking studies was done by Schrodinger program Maestro 10.5 software. The study is to observe the molecular binding pattern of the different natural biomarkers within the active pocket of the crystal structure of peroxisome proliferated activated receptor (PPAR-γ; PDB ID: 1FM9). The docking data are presented in Table: 1. Charantin showed the highest docking score -9.407 in the active pocket of the PPAR-γ in comparison to that of other biomarkers. In the **(Fig. 1)** the details dock pose of the binding mode of charantin are expressed.

Table: 1. Docking score and binding free energy of selected biomarkers.

Compound name	**Docking Score**	**Binding free energy** (kcal/mol)
Aloin	-7.101	-48.63
Azadirachtin	-6.435	-41.61
Berberine	-8.813	-46.28
Betulin	-6.504	-44.37
Ceminic Acid	-8.108	-43.77

Charantin	-9.407	-53.73
Cucurbitacin	-7.060	-49.29
Curcumin	-7.950	-48.11
Gallic Acid	-6.402	-43.55
Gymnemic Acid	-9.083	-43.11
Mangiferine	-7.210	-35.93
Neringin	-8.461	-46.02
Piperine	-6.245	-41.28
Pterostilbene	-8.288	-39.18
Withaferin	-6.997	-44.99

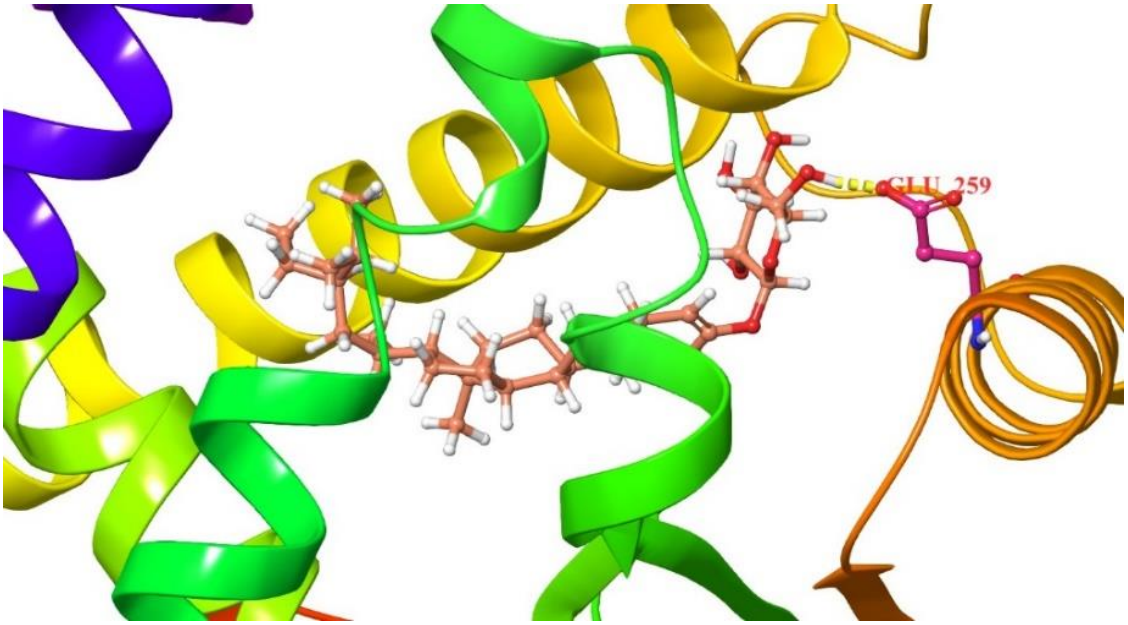

Fig. 1: 3D Docked posed conformer of Charantin (CRT)

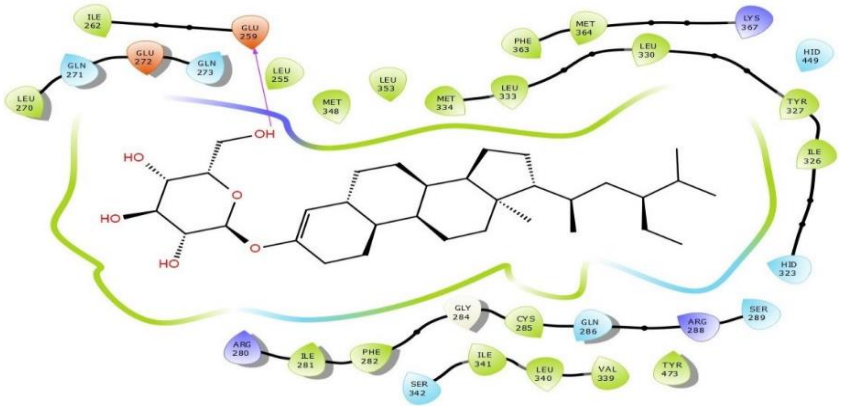

Fig. 2: 2D view of Charantin (CRT)

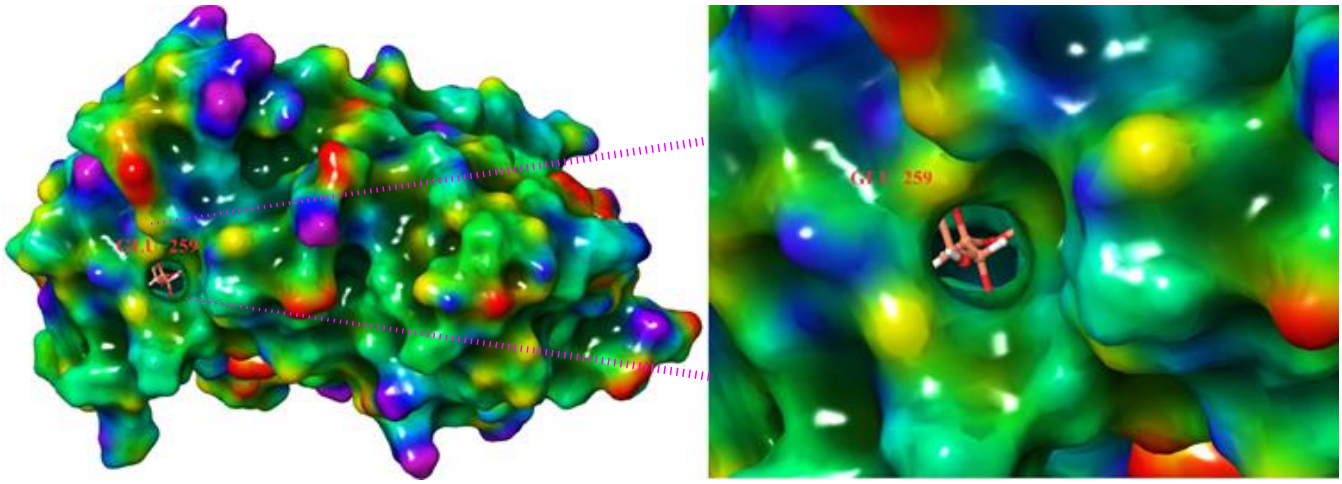

Fig. 3: Docked posed conformer of Charantin (CRT)

3.1.2. MM-GBSA binding free energy:

The binding free energy (ΔG) was estimated with Prime MM-GBSA by the Maestro 10.5 (Schrodinger Inc. USA) software. Then binding energies are depicted in (Table: 1.) showing that biomarker named "Charantin (CRT)" fit into the active pocket of the crystal structure of peroxisome proliferated activated receptor (PPAR-γ; PDB ID: 1FM9). The (ΔG) of taken compounds (biomarker of natural origin) are in the range of -53.73 to -39.18 kcal/mol, out of all, CRT is highest with (-53.73 kcal/mol) (ΔG).

3.2. Drug Characterization:

The sample of Charantin was "White Crystalline powder, Odourless, Tasteless. Its Melting point was recorded as: 268-270°C (Melting point apparatus). MW= 548.41; Rf Value: 0.54 (TEF- 5:4:1). The λmax of CRT in was found to be 276 nm. Its FTIR Scanning exhibit characteristics absorption bands {FT-IR (υ max, cm -1, KBr): 3526-3332 (O-Hstr), 1231 (C-Ostr), 3024 (C-Hstr), 2976 (C=Cstr), 1861 (C-Cstr), 1332 (C-O-Cstr)}.

3.2.1. HPLC chromatogram of Charantin:

HPLC chromatogram of Charantin (CRT) is shown in Fig. 4**.**

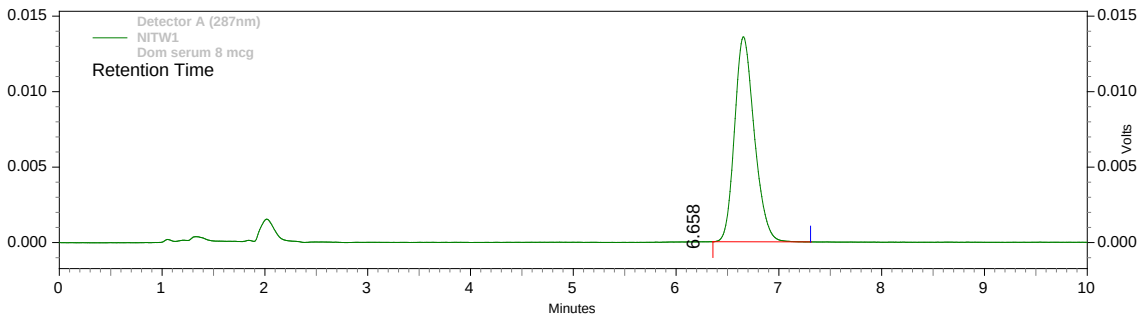

Fig. 4: Representative HPLC chromatogram of Charantin in mobile phase

3.2.2. RP-HPLC of drug (CRT):

The mobile phase (75:25 v/v) was used at a 1.2 mL/min rate. The optimum separation of CRT at 25 ± 0.5°C was found under the isocratic conditions. The Rt of CRT was found to be 6.65± 0.01 min (Fig. 4). A concentration (2-20 µg /mL) versus peak area graph was plotted, in this a good linear precision relationship is obtained as the correlation coefficient (r^2) of 0.9999 ± 0.01 **(**Fig. 5) (Attar and Ghane 2018).

SD = Standard deviation **RSD =** Regressed standard deviation

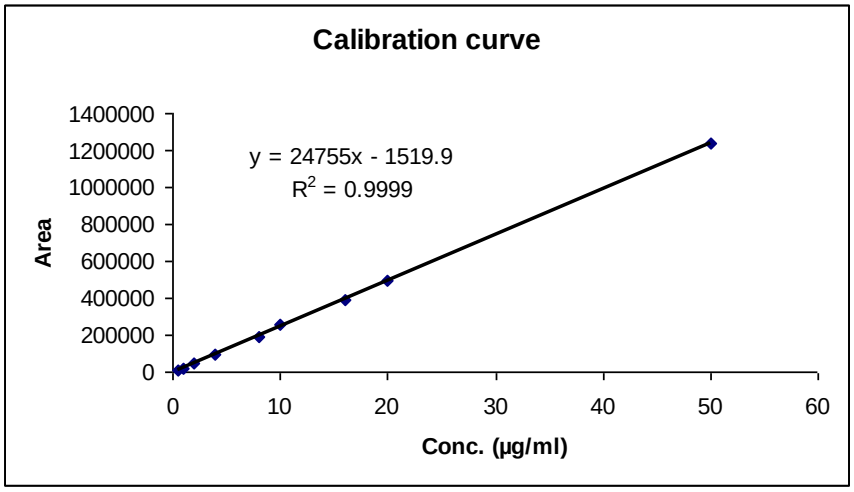

Fig. 5: Calibration curve in mobile phase for CRT by RP-HPLC method

3.3. Screening of Excipients & formulation of NEs:

Higher solubility of CRT in oil phase is required for nanoemulsion to maintain maximum drug in solubilised form in minimum volume of dispersed phase of nanoemulsion (NE). The drug CRT gave significant solubility (131.34±2.94, mean=3) in Sefsol 218, was selected as the oil phase, in water it was sparingly soluble (Fig.6).

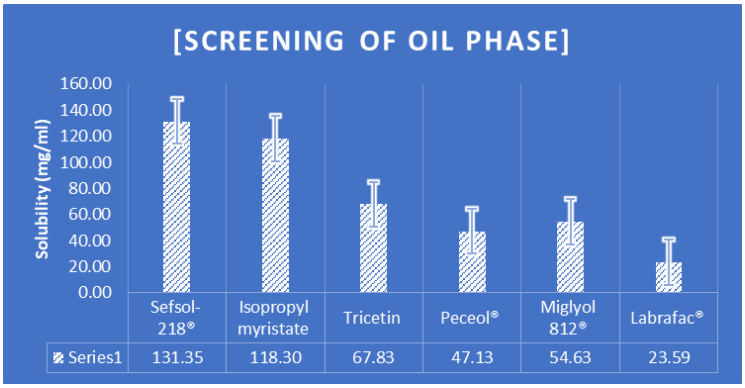

Fig. 6: CRT Solubility in different oils. (Mean ± SEM, n = 3).

Surfactant selection was based on its power of emulsification and solubilisation of selected oil (Sefsol-218). The criteria of GRAS (generally regarded as safe) & pharmaceutically acceptable was used.

Selection of co-surfactant and optimisation of its ratio was done to decrease the concentration of surfactant and ultimately fulfil criteria like safety, non-irritancy and non-sensitizing of formulation on skin. Drug solubility was analysed in different surfactants and co-surfactants and on the basis of transparency, Tween 80 & Transcutol, Tween 80 & Plurol oleique are selected as emulsifiers for placebo formulations (Table:2). The Required Hydrophilic Lipophilic Balance (RHLB) for o/w emulsion is greater than 10 (Craig et al. 1995). This RHLB was achieved by formation of mixed blend of surfactant and co-surfactants. Optimisation of ratio was done based on nanoemulsion available region (NEAR) on phase diagram.

Table: 2. Solubility of drug in various surfactants, co-surfactants

S No.	Surfactants	Observation	Solubility Rating
1.	Labrasol	Turbid	(**)
2.	Cremophore RH	Hazy and thick	(*)
3.	Cremophore EL	Clear solution	(*****)
4.	Tween 20	Clear solution	(*******)
5.	Tween 80	Clear yellow solution	(**********)
Co-surfactants			
1.	Transcutol	Clear	(**********)
2.	Plurol oleique	Clear	(**********)
3.	Propylene Glycol	Clear	(********)
4.	Methanol	Clear	(**********)

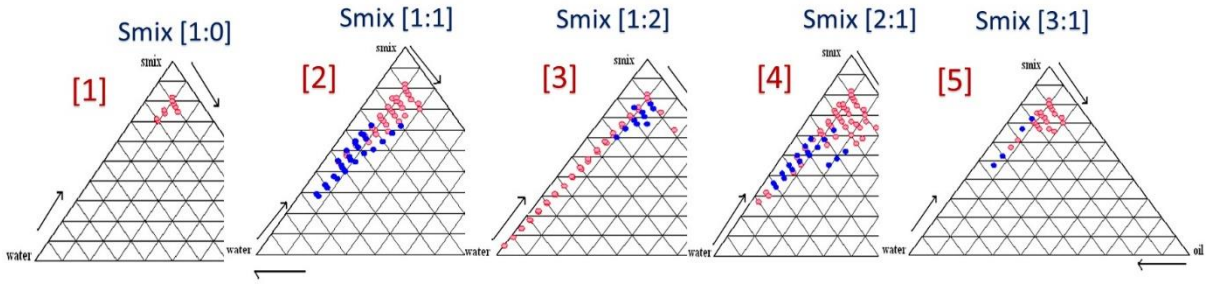

Fig. 7: (A-E). Pseudo-ternary-phase diagrams (PTP-Diagrams) expressing NEAR for Smix ratios.

NEs with optimum ratios of phases (oil +Smix+ Water) that is optimum ratios of components of emulsions was traced by PTP-diagram. Out of these the NEs with clear, transparent, having flow ability and required quantity of CRT can be loaded (Azeem, Ahmad, et al. 2009).

3.4. Optimisation of Formulation:

3.4.1. Thermodynamic Stability Study:

NEs were examined for thermodynamic stability (Table: 3.) by-Heating cooling cycle (H/C), Freeze thaw cycle (F/Th) & Centrifugation(C/f) (S. Alam et al. 2010) (Mostafa et al. 2015).

Table: 3. Composition of Stable & Selected NEs

Smix S:CoS	% Oil (v/v)	% S_{mix} (v/v)	% Water (v/v)	C/f	F/Th	H/C	Codes
1:1 (HLB-9.6)	22.85	29.3	47.85	√	√	√	NE3F
	25.21	24.61	50.18	√	√	√	NE4F
	29.77	25.75	44.48	√	√	√	NE6F
2:1 (HLB- 11.4)	20.51	19.78	59.71	√	√	√	NE1G
	23.72	22.08	54.2	√	√	√	NE3G
	25.85	22.3	51.85	√	√	√	NE4G
	30.3	24.99	44.71	√	√	√	NE8G
	30.76	25.53	43.71	√	√	√	NE10G
3:1 (HLB-12.3)	18.6	27.9	53.48	√	√	√	NE2H
	20.51	30.78	48.71	√	√	√	NE3H
	22.85	34.3	42.85	√	√	√	NE5H

3.4.2. Z-Average, polydispersity index (PDI), Zeta-Potential(ζ) and viscosity(η) analysis:

The droplets of all NEs are in the nano range and these are uniformly dispersed, this is done on basis of low PDI values. The PDI of NE4G was (0.577) this lowest value signifies the presence of uniform- dispersion and ultimately highest stability of NE (Mustafa et al. 2012).

The size of particles with selected Smix ratios (1:1, 2:1, and 3:1) are shown in Table: 4. (Fig.8). NE4G with surfactant: Co-Surfactant = 2:1 has minimum droplet size (118.03±1.11nm) in the selected all formulations. The minimum will be the droplet size, maximum will be their total surface area to interact with and consequently the highest permeation flux was for NE4G i.e. (Jss= 0.319±0.011). NE4F with Smix =1:1 is second mini for droplet size (172.9±1.09 nm) and its permeation flux (Jss=0.295±0.022) is second to maximum and the size of particles of formulation NE2H containing Smix= 3:1 is third mini droplet size (188.0±1.13 nm) and its smallest with (Jss=0.262±0.033).

Table: 4. Z-Average, PDI, ζ – potential, and Viscosity (η) of the NEs (n=3)

Smix (S:CoS)	Codes	Z-Average Mean±SD (nm)	PDI	ζ - potential	η- Mean ± SD (Cp)
1:1 (HLB-9.6)	NE3F	198.3±1.17	0.730	-36.9	141.10 ± 1.13
	NE4F	172.9±1.09	0.635	-34.8	128.60 ± 2.33
	NE6F	198.5±1.18	0.633	-34.9	133.10 ± 2.23
2:1 (HLB- 11.4)	NE1G	165.6±3.06	0.737	-35.3	122.12 ± 1.33
	NE3G	168.5±3.11	0.737	-35.6	128.10 ± 1.46
	NE4G	118.03±1.11	0.577	-35.8	111.01 ± 1.41
	NE8G	158.2±5.55	0.677	-33.8	129.10 ± 1.37
	NE10G	144.6±9.91	0.918	-33.9	128.10 ± 1.37
	NE2H	188.0±1.13	0.614	-35.6	129.10 ± 1.36
	NE3H	193.3±11.04	0.715	-35.6	141.10 ± 1.39
	NE5H	198.3±11.04	0.717	-34.7	144.23 ±1.29

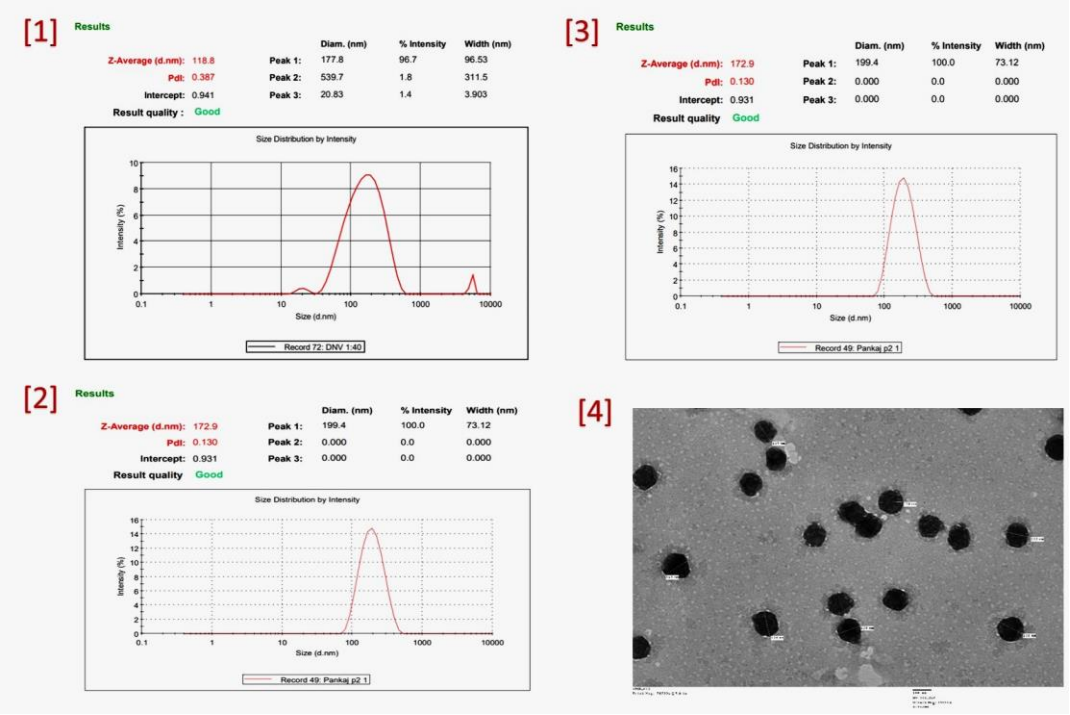

Fig. 8: (A-D). Z-average-Size distribution of- NE4G is (A), NE4F is (B), NE2H is (C) and TEM of NE is (D).

The values of ζ -potential & Viscosity are tabulated in table: 4 & in Fig. 8. The optimum value provides optimum repulsive forces between droplets that are responsible for stability. The ζ- potential was recorded in range of NEs (±33.8 mV to ±36.9). ζ- Potential of ±35.8 mV is reported for formulation NE4G. The optimum sufficient potential for stability of nanoemulsion of NEs was reported around ±50 mV.

Low Viscosity or good fluidity are the characteristics of NEs and due to lower viscosity NEs expresses Newtonian Flow (Azeem, Ahmad, et al. 2009).

The ζ- potential was recorded in range of NEs (±33.8 mV to ±36.9). ζ- potential of ±35.8 mV is reported for formulation NE4G. The optimum sufficient potential for stability of nanoemulsion of NEs was reported around ±50 mV.

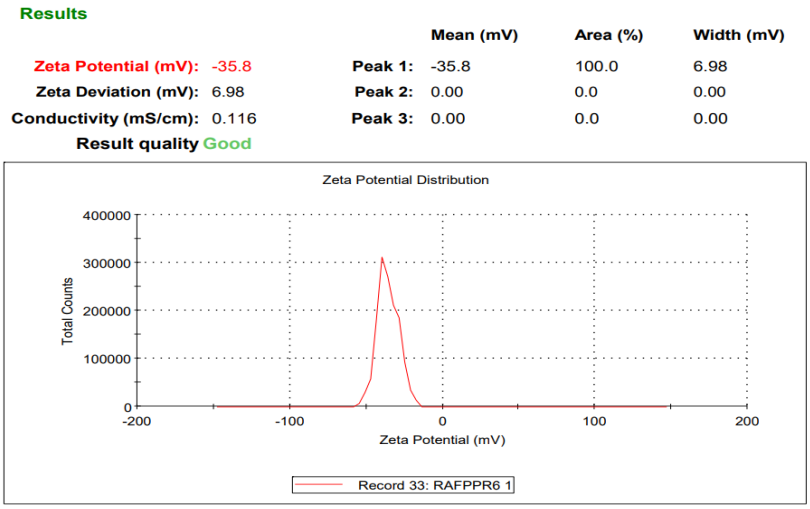

Fig. 9. Zeta (ζ)-Potential of droplet of NE4G Nanoemulsion.

3.4.3. Refractive Index (RI)

Table: 5. RI for Drug Loaded and Placebo Nanoemulsion (n = 3).

Smix (S:CoS)	Codes for Formulation	Drug loaded Refractive Index ± SD	Placebo Refractive Index ± SD
1:1 (HLB-9.6)	NE3F	1.391±0.006	1.381±0.007
	NE4F	1.388±0.006	1.384±0.006
	NE6F	1.399±0.007	1.387±0.006
2:1 (HLB- 11.4)	NE1G	1.383±0.005	1.381±0.007
	NE3G	1.385±0.005	1.382±0.004
	NE4G	1.387±0.005	1.385±0.004
	NE8G	1.398±0.005	1.386±0.005
	NE10G	1.391±0.006	1.389±0.007
3:1(HLB-12.3)	NE2H	1.395±0.004	1.381±0.004
	NE3H	1.387±0.006	1.883±0.006
	NE5H	1.381±0.008	1.885±0.006

The RI of drug loaded NE and of placebo are analysed, there were no significant differences between the two values (Table: 5). It signifies that the NEs were thermodynamically and chemically stable and remain isotropic after drug loading. There were no interactions between nanoemulsion excipients and drug.

3.4.4. In-vitro Drug entrapment (EE) & Drug Release Kinetics analysis:

Table: 6. Drug entrapment, drug release, R^2 values (n = 6), ensuring best fit release Model.

Smix (S:CoS)	Codes	Entrapment Efficiency (EE%)	Fraction of drug Released at 24th hr.	R^2 (Release w.r.t. to time)	Best Fit Model
1:1 (HLB-9.6)	NE3F	62.35±4.44	77.9±2.31	0.9736	HIGUCHI
	NE4F	78.42±1.33	95.9±1.28	0.9789	HIGUCHI
	NE6F	63.69±3.55	77.3±1.98	0.9714	HIGUCHI
2:1 (HLB-11.4)	NE1G	57.82±3.38	70.9±1.79	0.9193	HIGUCHI
	NE3G	68.23±3.72	77.8±1.67	0.9546	HIGUCHI
	NE4G	88.11±2.14	98.1±0.99	0.9883	HIGUCHI
	NE8G	72.42±2.36	69.8±1.93	0.9373	HIGUCHI
	NE10G	73.91±2.99	63.2±1.79	0.9562	HIGUCHI
3:1(HLB-12.3)	NE2H	70.77±3.39	92.8±0.98	0.9828	HIGUCHI
	NE3H	55.82±2.39	79.9±1.95	0.9676	HIGUCHI
	NE5H	51.91±2.93	73.3±1.02	0.9656	HIGUCHI

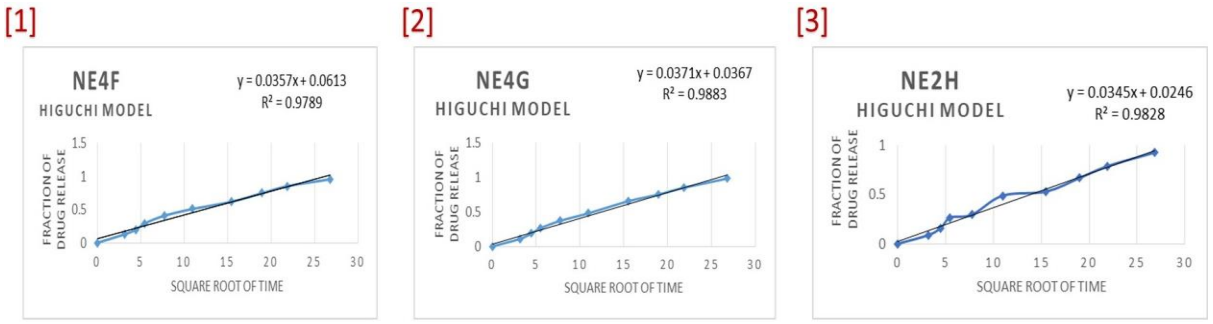

Fig. 10. (1 - 3). Release kinetics plots (Higuchi Model): (1) NE4F (B) NE4G (C) NE4H formulation.

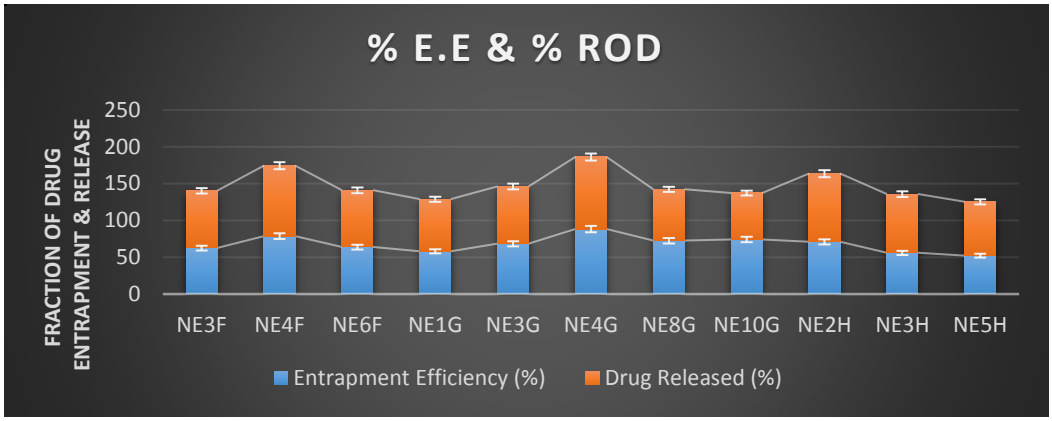

Fig. 11. Entrapment Efficiency (E.E) & Release of drug (ROD) from NEs

Dissolution studies to confirm release kinetics was done. R^2 values for each loaded with equal quantity of CRT (w/w) was evaluated. On the basis of $R^{2,}$ the best-fit model was reported as Higuchi Model of release (Table: 6) Fig.10. %EE and Fraction of drug Released **(FDR)** was

studied and recorded. NE4G showed best results so marked as optimised one. On second and third it was NE4F & NE2H.

3.4.5. CRT permeation study trough rat-skin:

Ex-vivo **P**ermeation profile via skin was obtained and compared to finalise the best optimised NE out of 11 different NEs. 3 Neat Formulations as NF^f (Smix-1:1), NF^g (Smix-2:1) & NF^h (Smix-3:1) was taken as control formulations for each Smix respectively (Table: 7. and Fig. 12.). All formulations were loaded with same quantity of drug w/w. The Permeation Flux (Jss) was taken as parameter for comparison and it was found that Flux of each Ne is significantly higher ($P<0.01$) than NF-Control. The enhancement ratio (ER) were significantly increased in NEs as compared with neat formulations this is because the particle size in NEs are of nano scale this facilitates penetration to maximum parts of ridges and furrow over skin and transporting the drug closest to skin-cells. As much as the size decreases the total effective surface area increases and huge surface area of NEs cover maximum permeation contact surface area and sites on skin. High solubilisation of drug exposes molecules of particles this facilitates faster release and permeation by diffusion. Hydrated skin supports faster penetration of drug which is achieved by external phase of NEs. **CDP** ($\mu g/cm^2$) of three best Formulations (n = 3)* out of 3 Smix groups are expressed in Table: 8. Fig. 13. NE4G formulation is selected as optimised one.

Table: 7. Permeability Parameter of CRT - Steady-state flux (Jss) and enhancement ratio (ER) w.r.t. (**NF^f**-control), (**NF^g**-control) and (**NF^g**-control). (Mean ± SD, n=3) *

Smix (S:CoS)	Formulation Codes	Jss ± SD ($mg/cm^2/h$)	ER
	NF^f (Neat Formulation)	**0.018±0.005**	1.00
1:1 (HLB-9.6)	NE3F	0.263±0.021	14.61
	NE4F	0.295±0.022	16.39
	NE6F	0.250±0.033	13.89
2:1 (HLB- 11.4)	**NF^g (**Neat Formulation)	**0.019±0.003**	1.00
	NE1G	0.246±0.022	12.95
	NE3G	0.277±0.019	14.58
	NE4G	0.319±0.011	16.79
	NE8G	0.271±0.023	14.26
	NE10G	0.235±0.022	12.37
3:1(HLB-12.3)	**NF^h (**Neat Formulation)	**0.019±0.004**	1.00
	NE2H	0.262±0.033	13.79
	NE3H	0.251±0.051	13.21
	NE5H	0.232±0.051	12.21

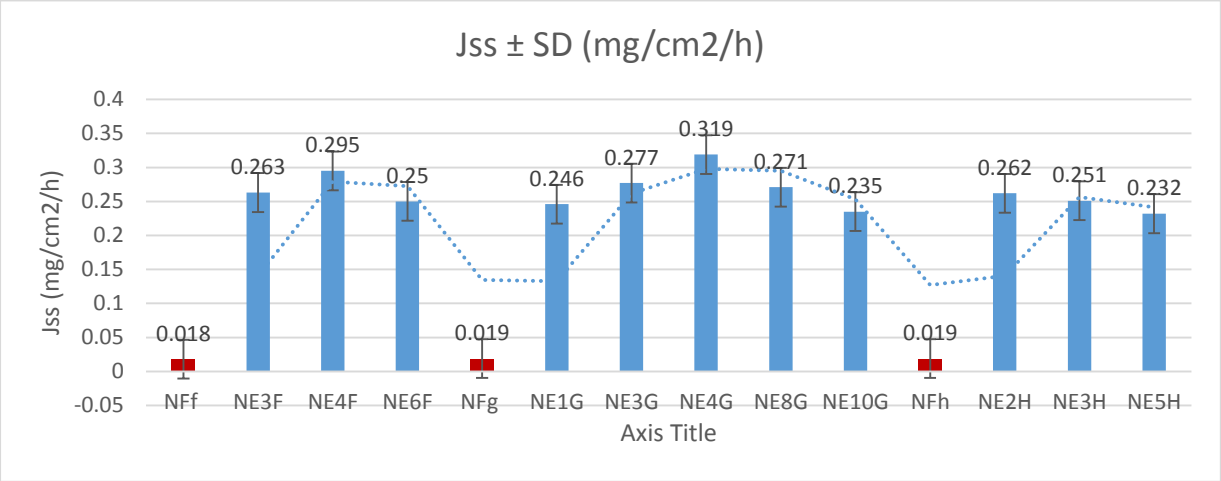

Fig. 12. EX-VIVO skin permeation analysis of drug with Permeation Flux (Jss) of NEs

Table 8. CDP (µg/cm^2) of Formulations selected.

CDP (µg/cm^2)			
Time (h)	**NE4F**	**NE4G**	**NE2H**
1	316.67	403.33	250.00
2	586.67	863.33	383.33
3	1163.33	1573.33	620.00
4	1670.00	2270.00	983.33
5	2253.33	2730.00	1290.00
6	2896.67	3563.33	1556.67
7	3303.33	4030.00	1896.67
8	4206.67	4803.33	2283.33
10	4690.00	5570.00	2623.33
12	5340.00	6673.33	4753.33
24	7090.00	7663.33	6296.67

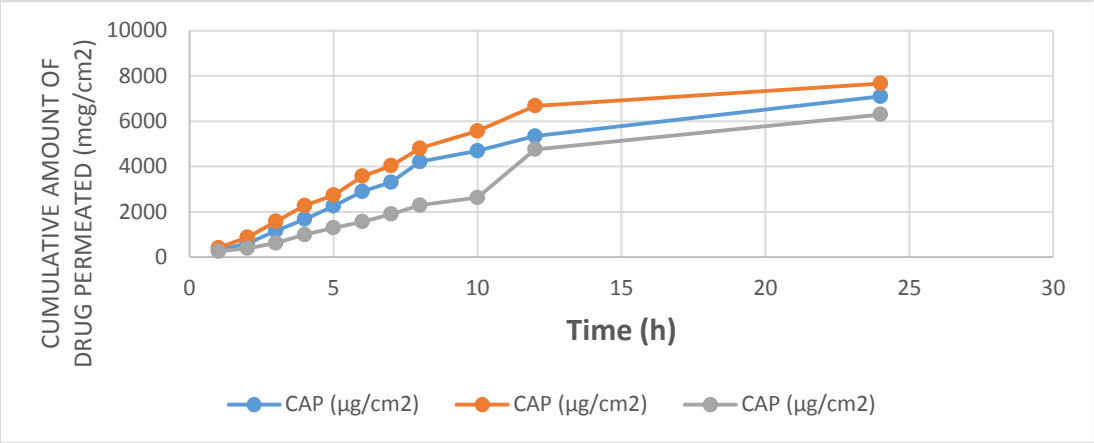

Fig. 13. EX-VIVO skin permeation profile of CRT from NEs.

3.5. TRANSFORMING OPTIMISED NE (NE4G) INTO NANOGEL :

Formulation characterization, drug entrapment, release and permeation through skin ascertained the CRT-NE4G as optimised one, this is decided to convert it in to gel by the use of 1% carbopol 934.

3.5.1. Ex-Vivo Permeation from CRT-NG:

Permeation of drug from CRT-NG, CRT-NE4G and NF^{cg} (loaded with equal amount of drug) was performed (mean ± SD, n=3)* (Table: 9. Fig. 14.). CRT-NG was observed best one to permeate the drug (CDP = 97.48%) than NF^{cg} (22.64%) and NE4G (91.96%) at 24^{th} hrs.

Table: 9. CDP & Jss {CRT-NG, CRT- NE4G, Conventional gel (NF^{cg})}. (Mean ± SD, n=3) *

Formulation Code	CDP (µg/cm^2)	CDP (%)	Jss ± SD (mg/cm^2/h)
CRT-NE4G	7663.33	91.96	0.319 ± **0**.01
CRT-NG	8123.33	97.48	0.339 ± **0**.086
NF^{cg}	1886.67	22.64	0.079 ± **0**.003

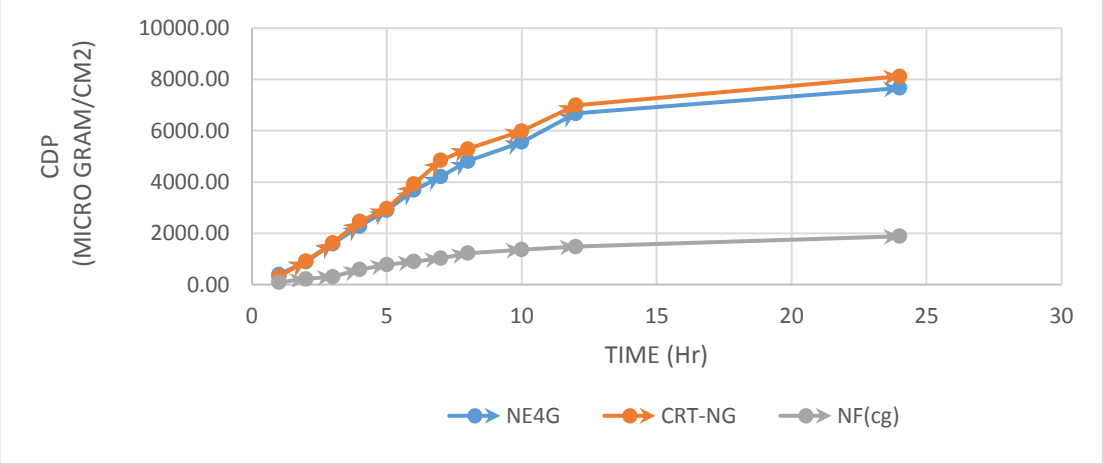

Fig. 14. Plot-In-comparison: Permeation Profile of NE4G, CRT-NG & NF^{cg} through rat skin.

3.5.2. Accelerated Stability Assessment of Nano-Gel:

Table: 10. Stability Studies of CRT-NG:

	Optimised Nanogel formulation (CRT-NG) containing 2% w/v of Drug															
							Storage condition									
SN	Parameters	25 °C ± 2 °C/60% RH ± 5% RH					32 °C ± 2 °C/60% RH ± 5% RH					40 °C ± 2 °C/75% RH ± 5% RH				
				Months				Months					Months			
		0	1	2	3	6	0	1	2	3	6	0	1	2	3	6
1	Colour	No change in color					No change in color					No change in color				
2	Odour	No change in odour					No change in odour					No change in odour				
3	Homogeniety			Smooth					Smooth					Smooth		
4	pH	6.48	6.45	6.43	6.38	6.34	6.48	6.46	6.42	6.39	6.35	6.48	6.46	6.41	6.38	6.34
5	Viscosity(Poise)	0.384	0.384	0.381	0.377	0.375	0.384	0.382	0.379	0.376	0.371	0.384	0.381	0.376	0.371	0.361
6	Net Content	99.3	98.5	98.1	97.9	97.5	99.2	99.2	98.1	97.7	97.5	99.3	98.1	97.3	95.2	95.1
7	Microbial load (Bacteria & Fungi)	No microbial growth was observed at 24, 48 and 72 h					No microbial growth was observed at 24, 48 and 72 h					No microbial growth was observed at 24, 48 and 72 h				
8	Sterility test	No microbial growth was observed at 24, 48 and 72 h					No microbial growth was observed at 24, 48 and 72 h					No microbial growth was observed at 24, 48 and 72 h				

It was observed that colour, odour, homogeneity, pH, viscosity and net content of drug in CRT-NG remain unchanged during testing period (0, 1, 2, 3 and 6 months). Results are significantly explaining the stability (Table: 10).

5. IN-VIVO STUDIES:

5.1. Antidiabetic Efficacy study of the CRT loaded Nanogel:

The data of blood glucose level of STZ-Induced-diabetic rats for 21 days treatment by Nanoemulsion based gel loaded with **drug** (CRT-NG) (Table:11, fig. 15.) was statistically analyzed, for its hypoglycemic effect and found statistically significant ($P<0.01$, Mean ± SEM); n=6) as compared with Standard Drug Gel (SD^g) and control group-II.

Table: 11. Data of blood glucose level of animals during 21 days treatment:

Groups	Treatment		Blood glucose level in mg/dl			
			1^{st} day	8^{st} day	14^{st} day	21^{st} day
I	Normal saline	NA	116.45±3.97 *	115.13±1.23 *	115.11±1.66 *	114.88±1.34 *
II	Diabetic control (streptozotocin)	50 mg/kg	367.83±4.15	372.45±2.16	377.53±2.99	389.63±3.36
III	Standard drug (SD^g)	100mg/kg	369.69±4.99	285.67±2.95 *	257.77±2.88 *	240.17±1.99 *
IV	Drug loaded Nano Gel (CRT-NG)	25 mg/kg	367.77±3.56	187.58±2.99 *	160.65±2.34 *	139.45±2.92 *
V	Drug loaded Nano Gel (CRT-NG)	50mg/kg	368.22±3.69	162.43±3.43 *	130.62±2.53 *	114.27±1.98 *

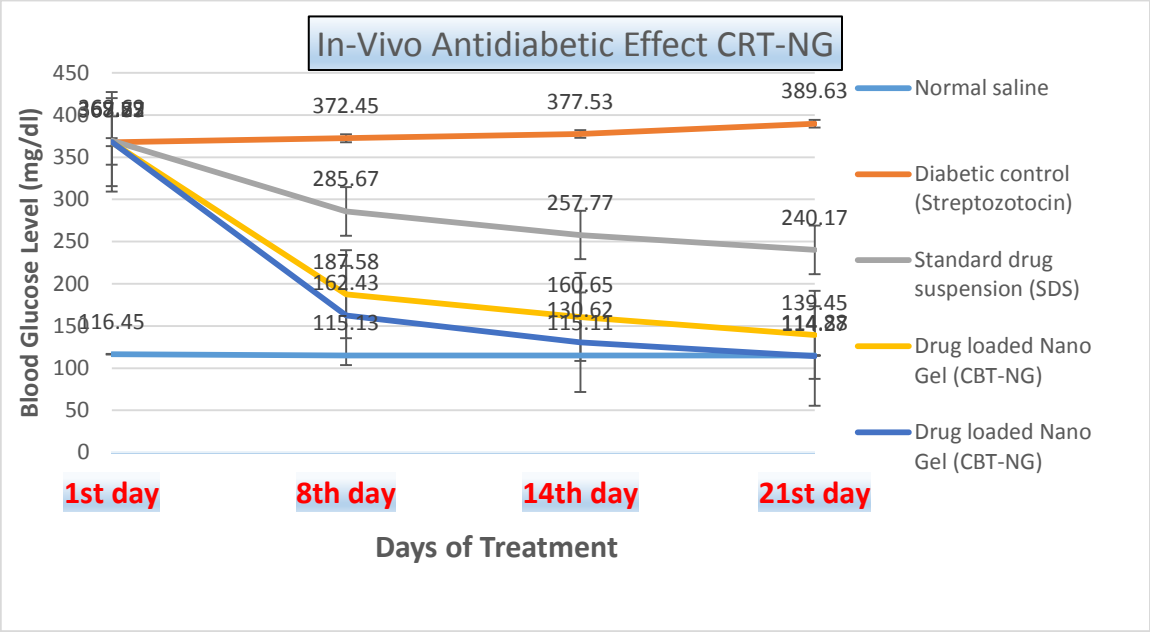

Fig. 15. Plot-In-Vivo Comparative study of Antidiabetic Activity of CRT-NG with SDS & Control.

5.2. Skin-irritancy test:

The statistical mean of irritancy score over rat skin after application of nanogel CRT-NG was found 1.25. (Table: 12 & 13). This data signifies that all additives/excipients used in CRT-NG were safe for topical application and TDDS.

Table: 12. Skin irritation score, (**A*** Erythema formation score. **B**** Oedema formation score)

Intact skin						Abraded skin				
	24 Hours		48 Hours				24 Hours		48 Hours	
Rats	A*	B**	A*	B**		Rats	A*	B**	A*	B**
1.	1	0	1	1		1.	0	1	1	1
2.	0	0	1	0		2.	1	0	2	0
3.	1	1	0	1		3.	0	2	1	1

Table: 13. Final skin irritation scores of CRT-NG (*= total of A and B from Part A; **= average of all skin reading of 24 and 48 hours)

Intact skin			Abraded skin		
Rats	(I)		(II)		Total Avg.(I + II)
	24 hours	48 hours	24 hours	48 hours	
1.	1	2	1	2	1.5**
2.	0	1	1	2	1**
3.	2	1	2	2	1.75**
Combined Average...					1.25**

CONCLUSION:

The concept of medication targeting in the systemic circulation while avoiding first pass metabolism is demonstrated and validated by the route of administration via transdermal delivery. Increased skin residence time from encapsulation in nanogel will result in superior therapeutics, improved dispersibility, and self-stabilised, as well as higher bioavailability and fewer side effects.

Comparing the available traditional preparation to the nanogel technology, the therapeutic dose and dosing frequency will reduce. The improved nanogel composition will help manage diabetes over the long term.

In order to boost the solubility and consequent transdermal flux of marginally water soluble anti-diabetic medications, it was suggested to develop a gel system based on a nanoemulsion. This will allow the drugs to exercise their effects directly through systemic circulation after entering in to the body.

Acknowledgement:

The Sharda University in Greater Noida helped the writers by providing free-Internet facility, national and international journals, and by supervising research works; they are appreciative. We also extend our gratitude to the R.V. N. I. for providing laboratories and other facilities necessary for performing research works.

Discloser:

The authors declare no financial gain or conflicts of interest related to this study.

References:

Aiyalu, Rajasekaran, Arulkumaran Govindarjan, and Arivukkarasu Ramasamy. 2016. "Formulation and Evaluation of Topical Herbal Gel for the Treatment of Arthritis in Animal Model." *Brazilian Journal of Pharmaceutical Sciences* 52 (3): 493–507. https://doi.org/10.1590/s1984-82502016000300015.

Alam, S., Z. Iqbal, A. Ali, R. K. Khar, F. J. Ahmad, S. Akhter, and S. Talegaonkar. 2010. "Microemulsion as a Potential Transdermal Carrier for Poorly Water Soluble Antifungal Drug Itraconazole." *Journal of Dispersion Science and Technology* 31 (1): 84–94. https://doi.org/10.1080/01932690903107265.

Alam, Sanjar, Zeenat I. Khan, Gulam Mustafa, Manish Kumar, Fakhrul Islam, Aseem Bhatnagar, and Farhan J. Ahmad. 2012. "Development and Evaluation of Thymoquinone-Encapsulated Chitosan Nanoparticles for Nose-to-Brain Targeting: A Pharmacoscintigraphic Study."

International Journal of Nanomedicine 7: 5705–18. https://doi.org/10.2147/IJN.S35329.

Arora, Swamita, Sangeetha Gupta, Wasim Akram, Ahmed E. Altyar, and Priti Tagde. 2023. "Effect of TLR3/DsRNA Complex Inhibitor on Poly(I:C)-Induced Airway Inflammation in Swiss Albino Mice." *Environmental Science and Pollution Research International* 30 (10): 28118–32. https://doi.org/10.1007/S11356-022-23987-6.

Attar, U. A., and S. G. Ghane. 2018. "Optimized Extraction of Anti-Cancer Compound – Cucurbitacin I and LC–MS Identification of Major Metabolites from Wild Bottle Gourd (Lagenaria Siceraria (Molina) Standl.)." *South African Journal of Botany* 119: 181–87. https://doi.org/10.1016/j.sajb.2018.09.006.

Azeem, Adnan, Farhan J. Ahmad, Roop K. Khar, and Sushama Talegaonkar. 2009. "Nanocarrier for the Transdermal Delivery of an Antiparkinsonian Drug." *AAPS PharmSciTech* 10 (4): 1093–1103. https://doi.org/10.1208/s12249-009-9306-2.

Azeem, Adnan, Mohammad Rizwan, Farhan J. Ahmad, Zeenat Iqbal, Roop K. Khar, M. Aqil, and Sushama Talegaonkar. 2009. "Nanoemulsion Components Screening and Selection: A Technical Note." *AAPS PharmSciTech* 10 (1): 69–76. https://doi.org/10.1208/s12249-008-9178-x.

Azeem, Adnan, Sushama Talegaonkar, Lalit M. Negi, Farhan J. Ahmad, Roop K. Khar, and Zeenat Iqbal. 2012. "Oil Based Nanocarrier System for Transdermal Delivery of Ropinirole: A Mechanistic, Pharmacokinetic and Biochemical Investigation." *International Journal of Pharmaceutics* 422 (1–2): 436–44. https://doi.org/10.1016/j.ijpharm.2011.10.039.

Barkat, Md Abul, Harshita, Iqbal Ahmad, Raisuddin Ali, Satya Prakash Singh, Faheem Hyder Pottoo, Sarwar Beg, and Farhan Jalees Ahmad. 2017. "Nanosuspension-Based Aloe Vera Gel of Silver Sulfadiazine with Improved Wound Healing Activity." *AAPS PharmSciTech* 18 (8): 3274–85. https://doi.org/10.1208/s12249-017-0817-y.

Bhutani, Rubina, Dharam Pal Pathak, Garima Kapoor, Asif Husain, and Md Azhar Iqbal. 2019. "Novel Hybrids of Benzothiazole-1,3,4-Oxadiazole-4-Thiazolidinone: Synthesis, in Silico ADME Study, Molecular Docking and in Vivo Anti-Diabetic Assessment." *Bioorganic Chemistry* 83 (October 2018): 6–19. https://doi.org/10.1016/j.bioorg.2018.10.025.

Bhutani, Rubina, Dharam Pal Pathak, Garima Kapoor, Asif Husain, Ravi Kant, and Md Azhar Iqbal. 2018. "Synthesis, Molecular Modelling Studies and ADME Prediction of Benzothiazole Clubbed Oxadiazole-Mannich Bases, and Evaluation of Their Anti-Diabetic Activity through in Vivo Model." *Bioorganic Chemistry* 77: 6–15. https://doi.org/10.1016/j.bioorg.2017.12.037.

Chaudhari, Pallavi M., and Madhavi A. Kuchekar. 2018. "Development and Evaluation of Nanoemulsion as a Carrier for Topical Delivery System by Box-Behnken Design." *Asian Journal of Pharmaceutical and Clinical Research* 11 (8): 286–93. https://doi.org/10.22159/ajpcr.2018.v11i8.26359.

Craig, D. Q.M., S. A. Barker, D. Banning, and S. W. Booth. 1995. "An Investigation into the

Mechanisms of Self-Emulsification Using Particle Size Analysis and Low Frequency Dielectric Spectroscopy." *International Journal of Pharmaceutics* 114 (1): 103–10. https://doi.org/10.1016/0378-5173(94)00222-Q.

Egan, Aoife M., and Seán F. Dinneen. 2014. "What Is Diabetes?" *Medicine (United Kingdom)* 42 (12): 679–81. https://doi.org/10.1016/j.mpmed.2014.09.005.

———. 2019. "What Is Diabetes?" *Medicine (United Kingdom)* 47 (1): 1–4. https://doi.org/10.1016/j.mpmed.2018.10.002.

Fernandes, Ana R., Elena Sanchez-Lopez, Tiago Dos Santos, Maria L. Garcia, Amelia M. Silva, and Eliana B. Souto. 2021. "Development and Characterization of Nanoemulsions for Ophthalmic Applications: Role of Cationic Surfactants." *Materials* 14 (24): 1–17. https://doi.org/10.3390/ma14247541.

Ganesan, Palanivel, Palanisamy Arulselvan, and Dong Kug Choi. 2017. "Phytobioactive Compound-Based Nanodelivery Systems for the Treatment of Type 2 Diabetes Mellitus - Current Status." *International Journal of Nanomedicine* 12: 1097–1111. https://doi.org/10.2147/IJN.S124601.

Gothai, Sivapragasam, Palanivel Ganesan, Shin Young Park, Sharida Fakurazi, Dong Kug Choi, and Palanisamy Arulselvan. 2016. "Natural Phyto-Bioactive Compounds for the Treatment of Type 2 Diabetes: Inflammation as a Target." *Nutrients* 8 (8). https://doi.org/10.3390/nu8080461.

Habtemariam, Solomon. 2019. "Type-2 Diabetes: Definition, Diagnosis and Significance." *Medicinal Foods as Potential Therapies for Type-2 Diabetes and Associated Diseases*, 3–10. https://doi.org/10.1016/b978-0-08-102922-0.00001-8.

Harwansh, Ranjit K., Pulok K. Mukherjee, Shiv Bahadur, and Rajarshi Biswas. 2015. "Enhanced Permeability of Ferulic Acid Loaded Nanoemulsion Based Gel through Skin against UVA Mediated Oxidative Stress." *Life Sciences* 141: 202–11. https://doi.org/10.1016/j.lfs.2015.10.001.

Husain, Asif, Medha Bhutani, Shazia Parveen, Shah Alam Khan, Aftab Ahmad, and Md Azhar Iqbal. 2021. "Synthesis, in Vitro Cytotoxicity, ADME, and Molecular Docking Studies of Benzimidazole-Bearing Furanone Derivatives." *Journal of the Chinese Chemical Society* 68 (2): 362–73. https://doi.org/10.1002/jccs.202000130.

Khursheed, Rubiya, Sachin Kumar Singh, Sheetu Wadhwa, Bhupinder Kapoor, Monica Gulati, Rajan Kumar, Arya Kadukkattil Ramanunny, Ankit Awasthi, and Kamal Dua. 2019. *Treatment Strategies against Diabetes: Success so Far and Challenges Ahead*. *European Journal of Pharmacology*. Vol. 862. Elsevier B.V. https://doi.org/10.1016/j.ejphar.2019.172625.

Mostafa, Dina Mahmoud, Ahmed Alaa Kassem, Marwa Hasanein Asfour, Sahar Youssef Al Okbi, Doha Abdou Mohamed, and Thanaa El Sayed Hamed. 2015. "Transdermal Cumin Essential Oil Nanoemulsions with Potent Antioxidant and Hepatoprotective Activities: In-Vitro and in-Vivo Evaluation." *Journal of Molecular Liquids* 212: 6–15.

https://doi.org/10.1016/j.molliq.2015.08.047.

Mustafa, Gulam, Zeenat Khan, Tripta Bansal, and Sushama Talegaonkar. 2012. "Preparation and Characterization of Oil in Water Nano-Reservoir Systems for Improved Oral Delivery of Atorvastatin." *Current Nanoscience* 5 (4): 428–40. https://doi.org/10.2174/157341309789377989.

Shakeel, Faiyaz, Sanjula Baboota, Alka Ahuja, Javed Ali, Mohammed Aqil, and Sheikh Shafiq. 2007. "Nanoemulsions as Vehicles for Transdermal Delivery of Aceclofenac." *AAPS PharmSciTech* 8 (4): 91–98. https://doi.org/10.1208/pt0804104.

Simona, Antal Diana, Ardelean Florina, Chis Aimee Rodica, Ollivier Evelyne, and Serban Maria-Corina. 2017. "Nanoscale Delivery Systems: Actual and Potential Applications in the Natural Products Industry." *Current Pharmaceutical Design* 23 (17): 2414–21. https://doi.org/10.2174/1381612823666170220155540.

Sultana, Shaheen, Sushma Talegaonkar, Aseem Bhatnagar, Farhan J. Ahmad, and Gaurav Mittal. 2012. "Optimization of Nifedipine Loaded Gastroretentive Microcapsules for Biliary Colic." *Asian Journal of Pharmaceutics* 6 (4): 295–306. https://doi.org/10.4103/0973-8398.107566.

World Health Organization. 2016. "Global Report on Diabetes." *Isbn* 978: 88. https://doi.org/ISBN 978 92 4 156525 7.